DMD Fast Forward. Published on February 22, 2018 as DOI: 10.1124/dmd.117.079624
This article has not been copyedited and formatted. The final version may differ from this version.

Apixaban and Rosuvastatin Pharmacokinetics in Nonalcoholic Fatty Liver Disease

Rommel G. Tirona, Zahra Kassam, Ruth Strapp, Mala Ramu, Catherine Zhu, Melissa Liu, Ute I. Schwarz, Richard B. Kim, Bandar Al-Judaibi and Melanie D. Beaton

Department of Physiology & Pharmacology (R.G.T., C.Z., U.I.S, R.B.K.), Division of Clinical Pharmacology, Department of Medicine (R.G.T., C.Z., M.L., U.I.S., R.B.K.), Department of Medical Imaging (Z.K.), Division of Gastroenterology, Department of Medicine (B.A-J., M.D.B.), University of Western Ontario, Lawson Health Research Institute (R.G.T., Z.K., R.S., M.R., U.I.S., R.B.K., M.D.B.), London, ON, Canada, Department of Medicine (B.A-J.), University of Rochester, Rochester, NY, USA

Running Title: Apixaban and Rosuvastatin PK in NAFLD

Corresponding Author:

Dr. Melanie D. Beaton

Division of Gastroenterology, Department of Medicine

University of Western Ontario

London Health Sciences Centre

339 Windermere Road

London, Ontario N6A 5A5, Canada

Email: melanie.beaton@lhsc.on.ca

Tel: 519 663 3344

Number of text pages: 32

Number of Figures: 3

Number of Tables: 5

Number of References: 52

Number of words in: Abstract - 160

Introduction - 629

Discussion - 1402

Abbreviations: NAFLD, nonalcoholic fatty liver disease; NASH, non-alcoholic steatohepatitis; AUC, area under the plasma concentration-time curve; C_{max}, maximum plasma concentration; T_{max}, time to maximum plasma concentration, $t_{1/2}$, half-life; CL_{renal},

renal clearance; X_{urine}, amount excreted in urine; MR, magnetic resonance; 4βHC, 4β-hydroxycholesterol; LC-MS/MS, liquid chromatography-tandem mass spectrometry; CYP, cytochrome P450; OATP, organic anion-transporting polypeptide; OAT, organic anion transporter; NTCP, sodium taurocholate co-transporting polypeptide, P-gp, P-glycoprotein; BCRP, breast cancer resistance protein; MRP, multidrug resistance protein; PNPLA3, patatin-like phosphatase domain containing 3.

Abstract

There is little known about the impact of nonalcoholic fatty liver disease (NAFLD) on drug metabolism and transport. We examined the pharmacokinetics of oral apixaban (2.5 mg) and rosuvastatin (5 mg) when administered simultaneously in subjects with magnetic resonance imaging-confirmed NAFLD (*N*=22) and healthy controls (*N*=12). The areas under the plasma concentration-time curve (AUC_{0-12}) for apixaban were not different between control and NAFLD subjects (671 and 545 ng/mL×hr, respectively; *P*=0.15). Similarly, the AUC_{0-12} for rosuvastatin did not differ between control and NAFLD groups (25.4 and 20.1 ng/mL×hr, respectively; *P*=0.28). Furthermore, hepatic fibrosis in NAFLD subjects was not associated with differences in apixaban or rosuvastatin pharmacokinetics. Decreased systemic exposures for both apixaban and rosuvastatin were associated with increased body weight (*P*<0.001 and *P*<0.05, respectively). In multivariable linear regression analyses, only participant weight but not NAFLD, age or *SLCO1B1*/*ABCG2*/*CYP3A5* genotypes, was associated with apixaban and rosuvastatin AUC_{0-12} (*P*<0.001 and *P*=0.06). NAFLD does not appear to affect the pharmacokinetics of apixaban or rosuvastatin.

Introduction

Nonalcoholic fatty liver disease (NAFLD) is the most common liver disease, affecting approximately 30% of adult North Americans (Sayiner et al., 2016). It is defined by hepatic steatosis, in the absence of significant alcohol consumption and other causes of hepatic fat accumulation (Ludwig et al., 1980). NAFLD encompasses both simple steatosis and non-alcoholic steatohepatitis (NASH), the latter being a more advanced stage of the disease, involving liver inflammation, hepatocyte ballooning and ultimately progressing to fibrosis (Brunt et al., 2011). NASH fibrosis is of particular concern as it is associated with increased liver-related and overall mortality (Dulai et al., 2017). There are no currently approved medications to treat NASH. Current disease management involves lifestyle modification and pharmacotherapies for common co-morbidities such as hypertension, diabetes and dyslipidemia (Rinella and Sanyal, 2016). A number of pharmacologic agents for NASH are being studied in clinical trials that aim to reverse the histologic features of the disease, particularly fibrosis (Rotman and Sanyal, 2017).

Despite the wide prevalence of NAFLD, it is remarkable that relatively little is known regarding how this disease influences drug disposition in humans. Few studies have evaluated the pharmacokinetics of drugs in NAFLD. In one study, antipyrine metabolic clearance was found to be reduced in NASH (Fiatarone et al., 1991), indicating lower overall cytochrome P450 (CYP) activity for the drug that is metabolized by multiple CYP isoenzymes (Engel et al., 1996). With respect to changes to particular CYP enzymes, it has been compellingly established that *in vivo* hepatic CYP2E1 activity is increased in

NASH, as revealed by chlorzoxazone phenotyping (Emery et al., 2003; Orellana et al., 2006). In addition, we demonstrated that CYP3A activity is decreased in NAFLD using a combination of oral midazolam phenotyping and measurement of plasma 4β-hydroxycholesterol (4βHC), an endogenous metabolic biomarker (Woolsey et al., 2015). This reduced *in vivo* CYP3A activity in NAFLD was recently confirmed using a translational systems pharmacology approach (Krauss et al., 2017). Lastly, there are now several studies demonstrating that the systemic exposure of glucuronide metabolites of drugs, namely acetaminophen and morphine, are increased in NASH (Barshop et al., 2011; Canet et al., 2015; Ferslew et al., 2015). These findings were attributed to increased hepatocyte basolateral membrane expression of Multidrug Resistance Protein (MRP) 3 and hepatocellular internalization of canalicular MRP2 (Hardwick et al., 2011; Canet et al., 2015). Taken together, there remains a paucity of information on NAFLD-related changes in pharmacokinetics and the potential associated clinical impacts on drug efficacy and harms.

In this study, we compared the pharmacokinetics of apixaban, a direct-acting oral anticoagulant, and rosuvastatin, an HMG-CoA reductase inhibitor, in healthy subjects and patients with NAFLD. These two medications were chosen for evaluation because 1) they are commonly prescribed in the NAFLD population, affording a degree of practical relevance and 2) they are drugs with well-characterized disposition pathways that may shed new insights to potential disease alterations in drug metabolizing enzyme and transporter activity. Indeed, apixaban is eliminated through hepatic metabolism by CYP3A4/5, biliary excretion, renal excretion (glomerular filtration) and intestinal secretion

(Raghavan et al., 2009; Wang et al., 2010). Apixaban is a substrate of the efflux transporters Breast Cancer Resistance Protein (BCRP) and P-glycoprotein (P-gp) (Zhang et al., 2013). Rosuvastatin is minimally metabolized and eliminated by biliary and renal secretion (Martin et al., 2003). It is a substrate of BCRP, MRP2, MRP4 and P-gp (Huang et al., 2006; Kitamura et al., 2008; Knauer et al., 2010) and the uptake transporters, Organic Anion Transporting Polypeptides (OATP) 1B1, OATP1B3, OATP2B1 and Sodium Taurocholate Co-transporting Polypeptide (NTCP) in liver (Ho et al., 2006), as well as Organic Anion Transporter 3 (OAT3) in kidney (Windass et al., 2007). Notably, rosuvastatin is used as an *in vivo* probe for drug interactions involving transporters, namely OATP1B1 and BCRP (Stopfer et al., 2016; Prueksaritanont et al., 2017).

Materials and Methods

Transepithelial flux of apixaban and rosuvastatin in polarized Caco-2 cells. Caco-2 cells were obtained from American Type Culture Collection ATCC (Manassas, VA) and cultured in DMEM supplemented with 50 µg/ml streptomycin, 50 U/mL penicillin, L-glutamine (2 mM) and 10% fetal bovine serum. For transepithelial flux experiments, cells were seeded on 0.4 µm pore size, cell (12-well) culture inserts (VWR International, Mississauga, ON) at a density of 90,000 cells/well and grown for 14 days with media changes every 2 days. Prior to the start of a transport experiment, the media was removed from each compartment (apical and basal), washed and replaced with Krebs-Henseleit Bicarbonate Buffer (KHB, pH 7.4). Transport was initiated after removal of KHB and replacement with 700 µL of KHB including apixaban (22 µM, Toronto Research Chemicals, Toronto, ON)) or [^{3}H]rosuvastatin (42 µM, American Radiolabeled Chemicals, St. Louis, MO) in the donor compartment. Apixaban (22 µM), rosuvastatin (42 µM), fumitremorgin C (5 µM) or verapamil (50 µM) were included in both the apical and basolateral compartments in separate wells. Cells were incubated at 37°C with 5% CO_2 in a humidified environment, and 25 µl aliquots were removed hourly from each compartment over 4 h. The concentration of apixaban in samples was determined by liquid chromatography-tandem mass spectrometry as detailed below. [^{3}H]rosuvastatin concentration was determined by liquid scintillation spectrometry (PerkinElmer TriCarb2900 TR, Walthm, MA).

Pharmacokinetic Study Subjects. Healthy individuals (control) and NAFLD patients provided informed written consent to participate in this study which was approved by the

Human Subjects Research Ethics Board at the University of Western Ontario. Studies were conducted in accordance with the ethical standards of the Helsinki Declaration of 1975 (as revised in 1983). Participants were enrolled after clinical assessment and evaluation of serum biochemistry and hematology. Inclusion criteria for the NAFLD group were age 18 years or older, diagnosis based on American Association for the Study of Liver Disease definition (Chalasani et al., 2012) and magnetic resonance imaging (MRI)-confirmed hepatic steatosis. Exclusion criteria were acute or chronic renal insufficiency, use of steatogenic medications, use of medications that inhibit or induce CYP3A, OATPs, BCRP or P-gp and refusal to discontinue grapefruit juice or herbal medicines that are CYP3A/P-gp inducers one week prior to the pharmacokinetic study.

MR imaging and MR elastography. All imaging was performed with the patient in the supine position, on a 1.5T MR imaging (MRI) scanner (Aera, Siemens, Erlangen, Germany).

MR Elastography Examination

A commercial pneumatic driver system (Resoundant, Mayo Clinic Foundation, Rochester, MN) was used to create mechanical waves that were introduced into the subject's liver. The passive driver was placed anteriorly over the patient's liver, centered at the level of the xiphoid process, and secured with an elastic belt. The passive driver was connected via a polyvinylchloride tube to the active driver which was placed outside the scan room to induce 60 *Hz* vibrations into the liver.

Acquisition sequences

(a) MR Elastography

Our institution's standard MR Elastography protocol was used. Initially, axial T2 HASTE images of the liver were acquired during inspiration. Based on these images, four sections of liver were selected by the radiologist for the MR Elastography portion of the study. Stiffness maps were generated using a standard inversion algorithm, and were displayed with a 95% confidence map. Mean stiffness measurements were calculated based on overall stiffness from each of the four sections acquired, using a manually drawn region of interest (ROI). The ROI was placed only on areas within the 95% confidence map. Average stiffness for each liver section, as well as overall liver stiffness, was then calculated.

(b) Fat-signal fraction

Chemical shift gradient echo imaging is used commonly for liver fat quantification. Decreased signal intensity of the liver on out-of-phase images in comparison relative to in-phase images, is characteristic of fatty infiltration. In this study, manual ROIs were placed over the liver on the acquired chemical shift images (in-phase and out-of-phase). Fat signal fraction (FSF) was calculated by using the following formula, which takes into account the net signal in liver on out of-phase images in comparison with in-phase images:

$$FSF = (SIP - SOP)/2(SIP)$$

where SIP is the net hepatic signal on in-phase images and SOP is the net hepatic signal on out-of-phase images (Ma et al., 2009).

Pharmacokinetic study. Within one month of MR imaging and MR elastography, subjects were admitted to the Centre for Clinical Investigation and Therapeutics (Lawson Health Research Institute, London, ON) after an overnight fast. Participants refrained from citrus juice or caffeine consumption 1 day prior to the pharmacokinetic study. Discontinuation of statins was requested for those prescribed beginning 3 days prior to the study day. At baseline, a morning blood sample was provided for measurement of 4β-hydroxycholesterol (4βHC) and extraction of DNA for genetic analysis. Rosuvastatin 5 mg (Crestor, AstraZeneca) and Apixaban 2.5 mg (Eliquis, Bristol Myers Squibb) was administered simultaneously by mouth in 100 mL of water. Prior to dosing and at 0.5, 1, 2, 4, 6, 8, 10 and 12 hours thereafter, blood samples were obtained through an indwelling venous catheter for ethylenediaminetetraacetic-acid plasma drug concentration analysis. Urine was collected *in toto* over 3 intervals (0-4hr, 4-8hr and 8-12hr) after dosing for assessment of renal drug excretion. Approximately 4 hours and 10 hours after dosing, participants were provided meals. Plasma and urine samples were stored at -80°C until analysis.

Apixaban and Rosuvastatin Analysis. Plasma and urine samples were analyzed by liquid chromatography-tandem mass spectrometry (LC-MS/MS) for apixaban and rosuvastatin concentrations. Apixaban, rosuvastatin and d6-Rosuvastatin were obtained from Toronto Research Chemicals (Toronto, ON). [13C, 2H7]-apixaban was purchased from Alsachim (Illkirch Graffenstaden, France). Plasma (50 μL) proteins were precipitated with acetonitrile (150 μL) containing d6-rosuvastatin (10 ng/mL) and [13C,2H7]-apixaban (50 ng/mL) and centrifuged at 13,000g for 10 min at 4°C. The resulting supernatant (175

DMD Fast Forward. Published on February 22, 2018 as DOI: 10.1124/dmd.117.079624
This article has not been copyedited and formatted. The final version may differ from this version.

μL) was dried in a SpeedVac at 60°C and reconstituted in 150 μL (0.1% formic acid in water/acetonitrile; 75%/25%) for injection into the liquid chromatograph (Agilent 1200, Agilent, Santa Clara, CA). Analytes were separated on a Hypersil Gold C18 column (50 x 5 mm, 5 μm; ThermoFisher Scientific, San Jose, CA) under gradient elution with 0.1% formic acid in water and acetonitrile. With heated electrospray ionization, mass spectrometric detection (TSQ Vantage, ThermoFisher Scientific) was performed in positive mode with mass transitions 482.2 → 258.1 *m/z*, 488.1 → 264.2 *m/z*, 460.1 → 443.3 *m/z* and 468.1 → 451.3 *m/z* for rosuvastatin d6-rosuvastatin, apixaban and [13C, 2H7]-apixaban, respectively. Calibration standards and quality controls were prepared in human plasma (BioreclamationIVT, Baltimore, MD) and processed as described above. Between-run precision (CV%) and bias (%) of quality controls for apixaban were <14% and <10%, respectively, while those for rosuvastatin were <12% and 10%, respectively.

4β-hydroxycholesterol (4βHC) analysis. 4βHC concentration in plasma was determined by the picolinic acid derivatization and electrospray ionization LC-MS/MS method of Honda *et al*. (Honda et al., 2008), as detailed in our previous report (Woolsey et al., 2016).

Genotyping. DNA was extracted from whole blood using MagNA Pure system (Roche Diagnostics, Laval, PQ). Single nucleotide polymorphism analysis was performed using Taqman Allelic Discrimination Assays (Viia7, Applied Biosystems, Foster City, CA) for *SLCO1B1* 388 A>G (rs2306283), *SLCO1B1* 521T>C (rs4149056), *ABCG2* 421 C>A (rs2231142), *CYP3A4*22* (rs35599367), *CYP3A5*3* (rs776746) and PNPLA3 I148M

(rs738409). These genetic variants were chosen for evaluation as they are known to influence apixaban (Ueshima et al., 2017) or rosuvastatin (Keskitalo et al., 2009; DeGorter et al., 2013) pharmacokinetics. For PNPLA3, the genotype is associated with risk for NAFLD (Romeo et al., 2008).

Pharmacokinetic calculations. Pharmacokinetic analysis was performed using model-independent methods. Area under the concentration-time curve to the last sampling time (AUC_{0-12}) was calculated using linear trapezoid method. $AUC_{0-\infty}$ was calculated as the sum of AUC_{0-12} and C_{12}/k, where C_{12} is the last sampled concentration and k is the elimination rate constant obtained from the regressed slope of ln-transformed terminal concentrations. Half-life ($t_{1/2}$) was determined from ln2/k. Maximal plasma concentration (C_{max}) and time to C_{max} (T_{max}) were obtained directly from the observed results. Renal clearance (CL_{renal}) was calculated as the amount of drug excreted in urine from 0 to 12 hours ($X_{urine,\ 0-12}$) divided by AUC_{0-12}.

Statistical analysis. Comparisons of demographics, serum biochemistry and pharmacokinetic parameters with subjects in the Control group and NAFLD groups were performed using two-tailed, unpaired Student's t-test or Chi-square test (Microsoft Excel, Microsoft, Redmond, WA). Univariate associations between subject weight and drug AUC_{0-12} were performed to obtain Pearson's correlation coefficients (ρ) using GraphPad Prism (GraphPad, La Jolla, CA). Multivariable linear regression analyses were performed to determine the contribution of covariates (NAFLD status, age, weight, *SLCO1B1, ABCG2* and *CYP3A5* genotypes) to apixaban and rosuvastatin AUC_{0-12} using SPSS

(v.23, IBM Analytics, Armonk, NY). In multivariable linear regression analyses, we used an additive model for genotypes.

DMD Fast Forward. Published on February 22, 2018 as DOI: 10.1124/dmd.117.079624
This article has not been copyedited and formatted. The final version may differ from this version.

Results

Apixaban and Rosuvastatin Transport Interactions in vitro.

We assessed the possibility that simultaneous oral administration of apixaban and rosuvastatin may result in mutual pharmacokinetic interactions using the in vitro Caco-2 model. The transport of apixaban (22 μM) across polarized Caco-2 cells grown in the two-compartment configuration in either the apical-to-basolateral (A-to-B) or basolateral-to-apical (B-to-A) directions were not affected by the presence of rosuvastatin (42 μM) applied to both compartments (Fig. 1A). In parallel experiments, the presence of fumitremorgin C (5 μM), a BCRP inhibitor, reduced both the (A-to-B) and (B-to-A) permeability of apixaban (Fig. 1A). Furthermore, the B-to-A flux of apixaban was attenuated by the presence of the P-gp inhibitor, verapamil (50 μM) (Fig. 1A). Our findings on the effects of BCRP and P-gp inhibitors on apixaban permeability in Caco-2 cells are similar to those reported previously (Zhang et al., 2013). Conversely, the presence of apixaban did not affect the transepithelial flux of rosuvastatin in both A-to-B and B-to-A directions (Fig. 1B). However, both fumitremorgin C and verapamil reduced the B-to-A transport of rosuvastatin (Fig. 1B). These results demonstrate a lack of mutual effects on bi-directional transport across Caco-2 cells for apixaban and rosuvastatin.

Cohort Characteristics. Twelve healthy control and 22 NAFLD subjects were enrolled in the pharmacokinetic study. Detailed participant characteristics are presented in Table 1. Magnetic resonance (MR) imaging was used to detect and quantify the degree of hepatic steatosis for inclusion of subjects into the control and NAFLD study groups. Fat signal fraction values of ≥ 0.1 were used as a cutoff value for the presence of hepatic

DMD Fast Forward. Published on February 22, 2018 as DOI: 10.1124/dmd.117.079624
This article has not been copyedited and formatted. The final version may differ from this version.

steatosis and inclusion into the NAFLD group. The NAFLD cohort was segregated into NAFLD-no fibrosis (*N*=11) and NAFLD-fibrosis (*N*=11) subgroups by the presence of fibrosis as determined from liver biopsy or a positive MR elastography result (mean liver stiffness $\geq$ 2.9 kPa). Participant age was similar between control and NAFLD groups. Females tended to be overrepresented in the control group (83%) than the NAFLD group (50%) (*P*=0.056). Subjects were Caucasian with the exception of one African-American participant in the control group. Total body weight, body mass index (BMI), waist circumference, and concentrations of serum biomarkers of liver function (alanine aminotransferase, aspartate aminotransferase, γ-glutamyltranspeptidase and alkaline phosphatase) were significantly greater in the NAFLD than control group (Table 1). Serum creatinine was similar between groups. In the NAFLD group, diabetes, hypertension and dyslipidemia were prevalent, with higher proportion of co-morbidities in the NAFLD-fibrosis than the NAFLD-no fibrosis subgroup. The allelic frequencies of the *SLCO1B1* 388A>G, *SLCO1B1* 521T>C and *CYP3A5*3* polymorphisms were similar between the NAFLD group and controls. No *CYP3A4*22* alleles were carried by any study participant. The decreased function *ABCG2* 421C>A polymorphism (Keskitalo et al., 2009) was found at a higher allelic frequency in the control than NAFLD group (*P*=0.012). Lastly, the patatin-like phosphatase domain containing 3 (PNPLA3) I148M variant previously associated with hepatic steatosis and NASH risk (Romeo et al., 2008), was at similar prevalence between the control and NAFLD groups.

Apixaban Pharmacokinetics. The mean plasma concentration-time profiles for apixaban in each study group are presented in Fig. 2A. Apixaban $AUC_{0\text{-}12}$, $AUC_{0\text{-}\infty}$ and

C_{max} were not different between the control and NAFLD groups, although there was trend towards lower values for these parameters in the NAFLD group (*P*=0.15, *P*=0.31 and *P*=0.13, respectively) (Table 2). T_{max}, $t_{1/2}$, $X_{urine\ 0\text{-}12}$ and CL_{renal} were similar between control the NAFLD groups (Table 2). Additionally, pharmacokinetic parameters were not different between either the NAFLD-no fibrosis or NAFLD-fibrosis subgroups and the control group (Table 2). Apixaban $AUC_{0\text{-}12}$ was strongly correlated with total body weight with univariate (*P*<0.001) (Fig. 3A) and multivariable linear regression analyses (Table 3). Neither NAFLD status, age, *CYP3A5* nor *BCRP* genotypes were associated with apixaban $AUC_{0\text{-}12}$ as indicated by multivariable linear regression analyses (Table 3).

Rosuvastatin Pharmacokinetics. Mean plasma concentration results for rosuvastatin are shown in Fig. 2B. Rosuvastatin $AUC_{0\text{-}12}$, $AUC_{0\text{-}\infty}$ and C_{max} were similar between control and NAFLD groups (Table 4). Furthermore, T_{max}, $t_{1/2}$, $X_{urine\ 0\text{-}12}$ and CL_{renal} were similar among study groups (Table 4). Pharmacokinetic parameters were not different between the control and either the NAFLD-no fibrosis or NAFLD-fibrosis subgroups (Table 4). With univariate comparison, there was a small but significant correlation between rosuvastatin $AUC_{0\text{-}12}$ and total body weight (*P*=0.035) (Fig. 3B) and a trend (*P*=0.06) with multivariable linear regression analysis (Table 5). Rosuvastatin $AUC_{0\text{-}12}$ was not associated with either NAFLD status, age, *SLCO1B1* or *ABCG2* genotypes with multivariable linear regression analysis (Table 5).

DMD Fast Forward. Published on February 22, 2018 as DOI: 10.1124/dmd.117.079624
This article has not been copyedited and formatted. The final version may differ from this version.

Discussion

Apixaban pharmacokinetics were not different between healthy control and NALFD subjects (Fig. 2A, Table 2). Previously, we found that CYP3A activity was moderately decreased in a separate NAFLD group (Woolsey et al., 2015). In the current cohort, we also observed reduced CYP3A activity in NAFLD as suggested by examination of plasma 4βHC concentrations (Table 1). These decreased 4βHC concentrations were most pronounced in the NASH-fibrosis subgroup. Thus, it could have been anticipated that apixaban AUC would be greater in NAFLD than in controls given that this anticoagulant is metabolized by CYP3A enzymes (Wang et al., 2010). It should be considered however, that CYP3A-mediated metabolism is not a dominant elimination pathway for apixaban as was evidenced by moderate increases (2-fold) in apixaban plasma AUC when co-administered with ketoconazole, a strong inhibitor of both CYP3A and P-gp (Frost et al., 2015). Approximately 27% of apixaban clearance occurs through glomerular filtration in the kidney (Raghavan et al., 2009) and we observed that the renal elimination pathway was not different among the control and NAFLD groups whose serum creatinine concentrations were also similar. We found that apixaban AUC strongly correlated with total body weight of subjects, with lower systemic exposure seen with increasing mass (Fig. 3A). This result confirms previous observations at the extremes of body weight (Upreti et al., 2013), demonstrating that apixaban clearance follows allometric principles. We are unable to discern from the pharmacokinetic results whether NAFLD is associated with alterations in intestinal absorption or biliary and/or intestinal secretion of apixaban which may have offset the observed reduction in CYP3A activity. Lastly, both *CYP3A5*3* and *ABCG2* 421C>A genetic variations were not associated with apixaban AUC in this

relatively small cohort despite that these genetic markers were recently linked to greater plasma trough concentrations in Japanese patients with atrial fibrillation (Ueshima et al., 2017). While we did not find differences in apixaban plasma pharmacokinetics, additional focused studies are necessary to examine whether NAFLD may have specific effects on intestinal absorption and individual organ elimination pathways.

Interestingly, rosuvastatin systemic exposure was similar between the control and NAFLD groups (Fig. 2B, Table 4) despite that there were reasons to expect otherwise. For example, NASH liver tissues have increased protein expression of OATP1B1 and reduced OATP1B3 (Clarke et al., 2014b). Furthermore, the expression of MRP3, MRP4, MRP5, P-gp and BCRP is increased in NASH (Hardwick et al., 2011). Although also up-regulated, MRP2 is internalized from the hepatocyte canalicular membrane in NASH (Canet et al., 2015). Furthermore, there is reduced protein glycosylation of OATPs and MRP2 in NASH that may influence transporter function (Clarke et al., 2017). These changes in liver transporter expression appear to have an effect on the pharmacokinetics of glucuronide metabolites of acetaminophen and morphine (Barshop et al., 2011; Canet et al., 2015; Ferslew et al., 2015). Lastly, in a rodent model of NASH, the systemic and liver disposition of simvastatin was altered, owing to down-regulation of hepatic Oatps (Clarke et al., 2014a). However, our current findings indicate that there is either a lack of functional changes in rosuvastatin transporters in NAFLD or that a complex interplay of altered activities of uptake and efflux transporters in different tissues results in no changes in rosuvastatin systemic exposure. In this regard, it can be considered that the efficiency of renal secretion (CL_{renal}) of rosuvastatin is unaffected by NAFLD (Table 4). Moreover,

the recovery of rosuvastatin in urine ($X_{urine\ 0\text{-}12}$) was similar between NAFLD subjects and controls (Table 4), indicating that NAFLD did not change bioavailabilty or the relative contribution of liver and kidney in the overall elimination. However, it is not certain whether hepatocyte intracellular concentrations and intrinsic biliary clearance of rosuvastatin differs in NAFLD given that these may be poorly reflected by the plasma concentrations. The genetic polymorphisms in *SLCO1B1* (521T>C) and *BCRP* (421C>A) are associated with increased rosuvastatin plasma concentrations (Pasanen et al., 2007; Keskitalo et al., 2009; DeGorter et al., 2013). However, this was not observed herein and likely a consequence of the relatively small cohort size. Other genetic markers that may be associated with rosuvastatin disposition were not examined. There was a modest correlation between rosuvastatin AUC and body weight (Fig. 3B). This result is in keeping with a pharmacokinetic study in children and adolescents that showed rosuvastatin oral clearance (CL/F) was associated with weight (Macpherson et al., 2016).

It is possible that the experimental strategy of simultaneous administration of apixaban and rosuvastatin may have masked the impacts of NAFLD on drug disposition. A pharmacokinetic drug-drug interaction between rosuvastatin and apixaban as a study complication was considered unlikely for a number of reasons. First, apixaban is not expected to inhibit rosuvastatin transporters including OATPs and P-gp at clinical doses (Zhang et al., 2013; Tsuruya et al., 2017). Moreover, rosuvastatin is not an inhibitor of CYP3A or P-gp (Martin et al., 2002; Sakaeda et al., 2006), proteins that impact apixaban pharmacokinetics. However, it remains a possibility that apixaban and rosuvastatin mutually interact with BCRP or MRP transporters. To assess potential interactions on

these efflux transporters, we examined the transcellular flux of both apixaban and rosuvastatin in the presence and absence of the alternate medication in the *in vitro* Caco-2 cell model (Fig. 1). We found a lack of mutual interactions between apixaban and rosuvastatin on bidirectional flux across the Caco-2 cells which express BCRP, MRPs and P-gp, lending support for the use of simultaneous drug administration in the pharmacokinetic study. Nevertheless, we used the lowest available commercial doses for apixaban (2.5 mg) and rosuvastatin (5 mg) for both safety reasons as well as to minimize a potential drug-drug interaction. The drug-interaction potential may be different at higher doses of apixaban and rosuvastatin.

MR imaging and MR elastography were used to quantify hepatic steatosis and fibrosis, respectively. Both techniques have been well-validated against liver biopsy, which is currently considered the gold-standard for assessment of the presence and severity of histologic features of NAFLD (Dulai et al., 2016). Whereas fibrosis can be accurately measured with elastography, assessment of hepatic inflammation (NASH) requires liver biopsy. In the absence of liver histology, we were therefore not able to distinguish precisely those NAFLD subjects with NASH but no fibrosis. Consequently, it is possible that the NAFLD-no fibrosis subgroup may be comprised of subjects with NASH in addition to those with only simple steatosis. Within the NAFLD-fibrosis subgroup, we are similarly unable to completely define those participants with NASH. As the presence of fibrosis is highly associated with steatohepatitis (McPherson et al., 2015), we expect that the majority of subjects in the NAFLD-fibrosis subgroup have NASH. Indeed, liver stiffness as measured by MR-elastography, has been proposed as a non-invasive method to

detect NASH (Chen et al., 2011). In the NAFLD subgroup analyses, the pharmacokinetics of apixaban and rosuvastatin were not different between subjects without or with fibrosis in comparison to controls. We suspect that no pharmacokinetic differences would also be apparent if the NAFLD group were stratified into simple steatosis and NASH subgroups.

The findings of this study may inform the safety profiles of apixaban and rosuvastatin in the NAFLD population. As with other direct-acting anticoagulants (Ruff et al., 2015), higher bleeding risk with apixaban will likely associated with increased plasma concentrations. NAFLD does not appear to alter the plasma concentration-anticoagulation response effects of apixaban (Bos et al., 2017). Given that the mean apixaban exposure was not greater in NAFLD compared to control subjects, the disease itself may not necessarily be a factor for determining bleeding risk or therapeutic dose. For rosuvastatin, increased plasma concentrations have been associated with risk for severe myopathy (Jacobson, 2006), however we found systemic exposures were not greater in NAFLD. While our results do not reveal whether rosuvastatin hepatocyte intracellular concentrations are affected by NAFLD, the use of statins in this population with low grade transaminitis appears safe from a hepatotoxicity perspective (Bril et al., 2017). It is important to note that our findings for apixaban and rosuvastatin in NAFLD should not be extrapolated to more advanced stages of the disease such as in NASH cirrhosis. Moreover, the current pharmacokinetic results do not permit conclusions to be drawn with respect to the influence of NAFLD on the pharmacodynamics of apixaban and rosuvastatin.

In conclusion, we demonstrate that the pharmacokinetics of apixaban and rosuvastatin are not affected by NAFLD. These findings provide additional insights to our understanding of pharmacological factors that may affect drug response and adverse effects in patients with this highly prevalent disease.

Authorship Contributions

Participated in research design: Tirona, Kassam, Kim, Beaton

Conducted experiments: Tirona, Kassam, Strapp, Ramu, Zhu, Liu, Schwarz, Al-Judaibi, Beaton

Performed data analysis: Tirona, Kassam, Beaton

Wrote or contributed to the writing of the manuscript: Tirona, Kassam, Beaton

References

Barshop NJ, Capparelli EV, Sirlin CB, Schwimmer JB, and Lavine JE (2011) Acetaminophen pharmacokinetics in children with nonalcoholic fatty liver disease. *J Pediatr Gastroenterol Nutr* **52:**198-202.

Bos S, Potze W, Siddiqui MS, Boyett SL, Adelmeijer J, Daita K, Lisman T, and Sanyal AJ (2017) Changes of in vitro potency of anticoagulant drugs are similar between patients with cirrhosis due to alcohol or non-alcoholic fatty liver disease. *Thromb Res* **150:**41-43.

Bril F, Portillo Sanchez P, Lomonaco R, Orsak B, Hecht J, Tio F, and Cusi K (2017) Liver Safety of Statins in Prediabetes or T2DM and Nonalcoholic Steatohepatitis: Post Hoc Analysis of a Randomized Trial. *J Clin Endocrinol Metab* **102:**2950-2961.

Brunt EM, Kleiner DE, Wilson LA, Belt P, Neuschwander-Tetri BA, and Network NCR (2011) Nonalcoholic fatty liver disease (NAFLD) activity score and the histopathologic diagnosis in NAFLD: distinct clinicopathologic meanings. *Hepatology* **53:**810-820.

Canet MJ, Merrell MD, Hardwick RN, Bataille AM, Campion SN, Ferreira DW, Xanthakos SA, Manautou JE, HH AK, Erickson RP, and Cherrington NJ (2015) Altered regulation of hepatic efflux transporters disrupts acetaminophen disposition in pediatric nonalcoholic steatohepatitis. *Drug Metab Dispos* **43:**829-835.

Chalasani N, Younossi Z, Lavine JE, Diehl AM, Brunt EM, Cusi K, Charlton M, Sanyal AJ, American Gastroenterological A, American Association for the Study of Liver D, and American College of G (2012) The diagnosis and management of

non-alcoholic fatty liver disease: practice guideline by the American Gastroenterological Association, American Association for the Study of Liver Diseases, and American College of Gastroenterology. *Gastroenterology* **142:**1592-1609.

Chen J, Talwalkar JA, Yin M, Glaser KJ, Sanderson SO, and Ehman RL (2011) Early detection of nonalcoholic steatohepatitis in patients with nonalcoholic fatty liver disease by using MR elastography. *Radiology* **259:**749-756.

Clarke JD, Hardwick RN, Lake AD, Canet MJ, and Cherrington NJ (2014a) Experimental nonalcoholic steatohepatitis increases exposure to simvastatin hydroxy acid by decreasing hepatic organic anion transporting polypeptide expression. *J Pharmacol Exp Ther* **348:**452-458.

Clarke JD, Hardwick RN, Lake AD, Lickteig AJ, Goedken MJ, Klaassen CD, and Cherrington NJ (2014b) Synergistic interaction between genetics and disease on pravastatin disposition. *J Hepatol* **61:**139-147.

Clarke JD, Novak P, Lake AD, Hardwick RN, and Cherrington NJ (2017) Impaired N-linked glycosylation of uptake and efflux transporters in human non-alcoholic fatty liver disease. *Liver Int* **37:**1074-1081.

DeGorter MK, Tirona RG, Schwarz UI, Choi YH, Dresser GK, Suskin N, Myers K, Zou G, Iwuchukwu O, Wei WQ, Wilke RA, Hegele RA, and Kim RB (2013) Clinical and pharmacogenetic predictors of circulating atorvastatin and rosuvastatin concentrations in routine clinical care. *Circ Cardiovasc Genet* **6:**400-408.

Dulai PS, Singh S, Patel J, Soni M, Prokop LJ, Younossi Z, Sebastiani G, Ekstedt M, Hagstrom H, Nasr P, Stal P, Wong VW, Kechagias S, Hultcrantz R, and Loomba

R (2017) Increased risk of mortality by fibrosis stage in nonalcoholic fatty liver disease: Systematic review and meta-analysis. *Hepatology* **65:**1557-1565.

Dulai PS, Sirlin CB, and Loomba R (2016) MRI and MRE for non-invasive quantitative assessment of hepatic steatosis and fibrosis in NAFLD and NASH: Clinical trials to clinical practice. *J Hepatol* **65:**1006-1016.

Emery MG, Fisher JM, Chien JY, Kharasch ED, Dellinger EP, Kowdley KV, and Thummel KE (2003) CYP2E1 activity before and after weight loss in morbidly obese subjects with nonalcoholic fatty liver disease. *Hepatology* **38:**428-435.

Engel G, Hofmann U, Heidemann H, Cosme J, and Eichelbaum M (1996) Antipyrine as a probe for human oxidative drug metabolism: identification of the cytochrome P450 enzymes catalyzing 4-hydroxyantipyrine, 3-hydroxymethylantipyrine, and norantipyrine formation. *Clin Pharmacol Ther* **59:**613-623.

Ferslew BC, Johnston CK, Tsakalozou E, Bridges AS, Paine MF, Jia W, Stewart PW, Barritt ASt, and Brouwer KL (2015) Altered morphine glucuronide and bile acid disposition in patients with nonalcoholic steatohepatitis. *Clin Pharmacol Ther* **97:**419-427.

Fiatarone JR, Coverdale SA, Batey RG, and Farrell GC (1991) Non-alcoholic steatohepatitis: impaired antipyrine metabolism and hypertriglyceridaemia may be clues to its pathogenesis. *J Gastroenterol Hepatol* **6:**585-590.

Frost CE, Byon W, Song Y, Wang J, Schuster AE, Boyd RA, Zhang D, Yu Z, Dias C, Shenker A, and LaCreta F (2015) Effect of ketoconazole and diltiazem on the pharmacokinetics of apixaban, an oral direct factor Xa inhibitor. *Br J Clin Pharmacol* **79:**838-846.

Hardwick RN, Fisher CD, Canet MJ, Scheffer GL, and Cherrington NJ (2011) Variations in ATP-binding cassette transporter regulation during the progression of human nonalcoholic fatty liver disease. *Drug Metab Dispos* **39:**2395-2402.

Ho RH, Tirona RG, Leake BF, Glaeser H, Lee W, Lemke CJ, Wang Y, and Kim RB (2006) Drug and bile acid transporters in rosuvastatin hepatic uptake: function, expression, and pharmacogenetics. *Gastroenterology* **130:**1793-1806.

Honda A, Yamashita K, Miyazaki H, Shirai M, Ikegami T, Xu G, Numazawa M, Hara T, and Matsuzaki Y (2008) Highly sensitive analysis of sterol profiles in human serum by LC-ESI-MS/MS. *J Lipid Res* **49:**2063-2073.

Huang L, Wang Y, and Grimm S (2006) ATP-dependent transport of rosuvastatin in membrane vesicles expressing breast cancer resistance protein. *Drug Metab Dispos* **34:**738-742.

Jacobson TA (2006) Statin safety: lessons from new drug applications for marketed statins. *Am J Cardiol* **97:**44C-51C.

Keskitalo JE, Zolk O, Fromm MF, Kurkinen KJ, Neuvonen PJ, and Niemi M (2009) ABCG2 polymorphism markedly affects the pharmacokinetics of atorvastatin and rosuvastatin. *Clin Pharmacol Ther* **86:**197-203.

Kitamura S, Maeda K, Wang Y, and Sugiyama Y (2008) Involvement of multiple transporters in the hepatobiliary transport of rosuvastatin. *Drug Metab Dispos* **36:**2014-2023.

Knauer MJ, Urquhart BL, Meyer zu Schwabedissen HE, Schwarz UI, Lemke CJ, Leake BF, Kim RB, and Tirona RG (2010) Human skeletal muscle drug transporters determine local exposure and toxicity of statins. *Circ Res* **106:**297-306.

Krauss M, Hofmann U, Schafmayer C, Igel S, Schlender J, Mueller C, Brosch M, von Schoenfels W, Erhart W, Schuppert A, Block M, Schaeffeler E, Boehmer G, Goerlitz L, Hoecker J, Lippert J, Kerb R, Hampe J, Kuepfer L, and Schwab M (2017) Translational learning from clinical studies predicts drug pharmacokinetics across patient populations. *NPJ Syst Biol Appl* **3:**11.

Ludwig J, Viggiano TR, McGill DB, and Oh BJ (1980) Nonalcoholic steatohepatitis: Mayo Clinic experiences with a hitherto unnamed disease. *Mayo Clin Proc* **55:**434-438.

Ma X, Holalkere NS, Kambadakone RA, Mino-Kenudson M, Hahn PF, and Sahani DV (2009) Imaging-based quantification of hepatic fat: methods and clinical applications. *Radiographics* **29:**1253-1277.

Macpherson M, Hamren B, Braamskamp MJ, Kastelein JJ, Lundstrom T, and Martin PD (2016) Population pharmacokinetics of rosuvastatin in pediatric patients with heterozygous familial hypercholesterolemia. *Eur J Clin Pharmacol* **72:**19-27.

Martin PD, Kemp J, Dane AL, Warwick MJ, and Schneck DW (2002) No effect of rosuvastatin on the pharmacokinetics of digoxin in healthy volunteers. *J Clin Pharmacol* **42:**1352-1357.

Martin PD, Warwick MJ, Dane AL, Hill SJ, Giles PB, Phillips PJ, and Lenz E (2003) Metabolism, excretion, and pharmacokinetics of rosuvastatin in healthy adult male volunteers. *Clin Ther* **25:**2822-2835.

McPherson S, Hardy T, Henderson E, Burt AD, Day CP, and Anstee QM (2015) Evidence of NAFLD progression from steatosis to fibrosing-steatohepatitis using paired biopsies: implications for prognosis and clinical management. *J Hepatol* **62:**1148-1155.

Orellana M, Rodrigo R, Varela N, Araya J, Poniachik J, Csendes A, Smok G, and Videla LA (2006) Relationship between in vivo chlorzoxazone hydroxylation, hepatic cytochrome P450 2E1 content and liver injury in obese non-alcoholic fatty liver disease patients. *Hepatol Res* **34:**57-63.

Pasanen MK, Fredrikson H, Neuvonen PJ, and Niemi M (2007) Different effects of SLCO1B1 polymorphism on the pharmacokinetics of atorvastatin and rosuvastatin. *Clin Pharmacol Ther* **82:**726-733.

Prueksaritanont T, Tatosian DA, Chu X, Railkar R, Evers R, Chavez-Eng C, Lutz R, Zeng W, Yabut J, Chan GH, Cai X, Latham AH, Hehman J, Stypinski D, Brejda J, Zhou C, Thornton B, Bateman KP, Fraser I, and Stoch SA (2017) Validation of a microdose probe drug cocktail for clinical drug interaction assessments for drug transporters and CYP3A. *Clin Pharmacol Ther* **101:**519-530.

Raghavan N, Frost CE, Yu Z, He K, Zhang H, Humphreys WG, Pinto D, Chen S, Bonacorsi S, Wong PC, and Zhang D (2009) Apixaban metabolism and pharmacokinetics after oral administration to humans. *Drug Metab Dispos* **37:**74-81.

Rinella ME and Sanyal AJ (2016) Management of NAFLD: a stage-based approach. *Nat Rev Gastroenterol Hepatol* **13:**196-205.

Romeo S, Kozlitina J, Xing C, Pertsemlidis A, Cox D, Pennacchio LA, Boerwinkle E, Cohen JC, and Hobbs HH (2008) Genetic variation in PNPLA3 confers susceptibility to nonalcoholic fatty liver disease. *Nat Genet* **40:**1461-1465.

Rotman Y and Sanyal AJ (2017) Current and upcoming pharmacotherapy for non-alcoholic fatty liver disease. *Gut* **66:**180-190.

Ruff CT, Giugliano RP, Braunwald E, Morrow DA, Murphy SA, Kuder JF, Deenadayalu N, Jarolim P, Betcher J, Shi M, Brown K, Patel I, Mercuri M, and Antman EM (2015) Association between edoxaban dose, concentration, anti-Factor Xa activity, and outcomes: an analysis of data from the randomised, double-blind ENGAGE AF-TIMI 48 trial. *Lancet* **385:**2288-2295.

Sakaeda T, Fujino H, Komoto C, Kakumoto M, Jin JS, Iwaki K, Nishiguchi K, Nakamura T, Okamura N, and Okumura K (2006) Effects of acid and lactone forms of eight HMG-CoA reductase inhibitors on CYP-mediated metabolism and MDR1-mediated transport. *Pharm Res* **23:**506-512.

Sayiner M, Koenig A, Henry L, and Younossi ZM (2016) Epidemiology of Nonalcoholic Fatty Liver Disease and Nonalcoholic Steatohepatitis in the United States and the Rest of the World. *Clin Liver Dis* **20:**205-214.

Stopfer P, Giessmann T, Hohl K, Sharma A, Ishiguro N, Taub ME, Zimdahl-Gelling H, Gansser D, Wein M, Ebner T, and Muller F (2016) Pharmacokinetic Evaluation of a Drug Transporter Cocktail Consisting of Digoxin, Furosemide, Metformin, and Rosuvastatin. *Clin Pharmacol Ther* **100:**259-267.

Tsuruya Y, Nakanishi T, Komori H, Wang X, Ishiguro N, Kito T, Ikukawa K, Kishimoto W, Ito S, Schaefer O, Ebner T, Yamamura N, Kusuhara H, and Tamai I (2017)

Different Involvement of OAT in Renal Disposition of Oral Anticoagulants Rivaroxaban, Dabigatran, and Apixaban. *J Pharm Sci* **106:**2524-2534.

Ueshima S, Hira D, Fujii R, Kimura Y, Tomitsuka C, Yamane T, Tabuchi Y, Ozawa T, Itoh H, Horie M, Terada T, and Katsura T (2017) Impact of ABCB1, ABCG2, and CYP3A5 polymorphisms on plasma trough concentrations of apixaban in Japanese patients with atrial fibrillation. *Pharmacogenet Genomics* **27:**329-336.

Upreti VV, Wang J, Barrett YC, Byon W, Boyd RA, Pursley J, LaCreta FP, and Frost CE (2013) Effect of extremes of body weight on the pharmacokinetics, pharmacodynamics, safety and tolerability of apixaban in healthy subjects. *Br J Clin Pharmacol* **76:**908-916.

Wang L, Zhang D, Raghavan N, Yao M, Ma L, Frost CE, Maxwell BD, Chen SY, He K, Goosen TC, Humphreys WG, and Grossman SJ (2010) In vitro assessment of metabolic drug-drug interaction potential of apixaban through cytochrome P450 phenotyping, inhibition, and induction studies. *Drug Metab Dispos* **38:**448-458.

Windass AS, Lowes S, Wang Y, and Brown CD (2007) The contribution of organic anion transporters OAT1 and OAT3 to the renal uptake of rosuvastatin. *J Pharmacol Exp Ther* **322:**1221-1227.

Woolsey SJ, Beaton MD, Choi YH, Dresser GK, Gryn SE, Kim RB, and Tirona RG (2016) Relationships between Endogenous Plasma Biomarkers of Constitutive Cytochrome P450 3A Activity and Single-Time-Point Oral Midazolam Microdose Phenotype in Healthy Subjects. *Basic Clin Pharmacol Toxicol* **118:**284-291.

Woolsey SJ, Mansell SE, Kim RB, Tirona RG, and Beaton MD (2015) CYP3A Activity and Expression in Nonalcoholic Fatty Liver Disease. *Drug Metab Dispos* **43:**1484-1490.

Zhang D, He K, Herbst JJ, Kolb J, Shou W, Wang L, Balimane PV, Han YH, Gan J, Frost CE, and Humphreys WG (2013) Characterization of efflux transporters involved in distribution and disposition of apixaban. *Drug Metab Dispos* **41:**827-835.

Footnotes:

This work was supported by the Canadian Institutes of Health Research [Grant MOP-136909].

Figure Legends

Figure 1 Apixaban and rosuvastatin interactions in Caco-2 cells. (**A**) Apixaban and (**B**) rosuvastatin apparent permeabilities (P_{app}) across polarized Caco-2 cells in the apical to basolateral (A to B) and basolateral to apical (B to A) directions. Apixaban and rosuvastatin directional flux was monitored in the absence or presence of rosuvastatin, apixaban, fumitremorgin C (BCRP inhibitor) or verapamil (P-gp inhibitor) applied to both basolateral and apical compartments. Data are presented as mean and S.D. (*N*=3). ***, P<0.001; ****, P<0.0001 when compared to control P_{app} using t-test.

Figure 2 Plasma concentration-time curves after simultaneous oral administration of (**A**) apixaban 2.5 mg and (**B**) rosuvastatin 5 mg in healthy control subjects (open circles; *N*=12) and patients with NAFLD (closed circles; *N*=22). Data are presented as mean ± S.E.M.

Figure 3 Relationships between total body weight and AUC_{0-12} for (**A**) apixaban and (**B**) rosuvastatin in healthy control subjects (open circles; *N*=12) and patients with NAFLD (closed circles; *N*=22). Pearson's correlation coefficients (ρ), r^2 and *P*-value are noted.

Table 1. ***Participant characteristics.***

	Control (***N***=12)	**NAFLD** (***N***=22)	***P*-value***	**NAFLD No Fibrosis** (***N***=11)	***P*-value***	**NAFLD Fibrosis** (***N***=11)	***P*-value***
Age (yr)	46.0 ± 9.8	51.3 ± 12.4	0.18	50.9 ± 12.8	0.32	51.7 ± 12.5	0.24
Sex (Female - Male)	10 - 2	11 - 11	0.056	7 - 4	0.28	4 - 7	0.021
Weight (Kg)	65.6 ± 10.3	99.9 ± 21.9	<0.001	93.2 ± 23.5	0.003	106.6 ± 18.8	<0.001
BMI	23.4 ± 2.5	34.0 ± 4.5	<0.001	32.4 ± 3.9	<0.001	35.5 ± 4.8	<0.001
Waist Circumference (cm)	76.5 ± 5.0	111.4 ± 17.9	<0.001	109.5 ± 21.8	<0.001	113.1 ± 14.3	<0.001
ALT (U/L)	16.5 ± 7.5	49.4 ± 36.3	<0.001	49.1 ± 32.1	0.007	49.7 ± 41.6	0.024
AST (U/L)	24.0 ± 10.3	33.1 ± 15.5	0.048	30.6 ± 10.3	0.14	35.6 ± 19.6	0.10
GGT (U/L)	16.6 ± 6.3	52.1 ± 40.8	<0.001	43.8 ± 21.5	0.002	60.5 ± 53.6	0.02
Alk Phos (U/L)	61.3 ± 14.3	77.9 ± 18.1	0.006	79.1 ± 16.8	0.01	76.7 ± 20.1	0.05
Platelets (x10^9 cells/L)	234 ± 40	262 ± 75	0.16	261 ± 63	0.23	262 ± 89	0.34
Serum Creatinine (μM)	69.8 ± 13.8	67.8 ± 12.1	0.67	63.2 ± 11.5	0.23	71.9 ± 11.7	0.70
HgA1c (%)	5.3 ± 0.4	6.3 ± 0.9	<0.001	6.4 ± 1.0	0.004	6.2 ± 0.8	0.004
Diabetes	0/12	8/22	0.017	2/11	0.12	6/11	0.003
Hypertension	0/12	10/22	0.005	4/11	<0.001	6/11	0.003
Dyslipidemia	0/12	11/22	0.003	3/11	0.052	8/11	<0.001
MR fat signal fraction	-0.01 ± 0.05	0.27 ± 0.08	<0.001	0.30 ± 0.09	<0.001	0.24 ± 0.08	<0.001
4β-HC (ng/mL)	16.9 ± 3.2	11.9 ± 5.4	0.007	13.4 ± 5.9	0.13	10.4 ± 4.5	0.002
Genotypes[#] (Freq.%)							
SLCO1B1 388A>G	7/5/0 (21)	8/9/5 (43)	0.065	5/3/3 (41)	0.14	3/6/2 (46)	0.075
SLCO1B1 521T>C	8/4/0 (17)	15/7/0 (16)	0.935	7/4/0 (18)	0.89	8/3/0 (14)	0.78
ABCG2 421C>A	7/4/1 (25)	20/2/0 (5)	0.012	10/1/0 (5)	0.054	10/1/0 (5)	0.054
*CYP3A4*22*	12/0/0 (0)	22/0/0 (0)	-	11/0/0 (0)	-	11/0/0 (0)	-
*CYP3A5*3*	8/3/1 (79)	20/1/1 (93)	0.086	9/1/1 (86)	0.52	11/0/0 (100)	0.023
PNPLA3 I148M	9/3/0 (13)	12/8/2 (27)	0.16	5/5/1 (32)	0.11	7/3/1 (23)	0.36

Mean ± S.D.; [#] Genotype: Ref-Ref/Ref-Var/Var-Var, where Ref is carriers of reference allele and Var is variant allele; *two-tailed, t-test or Chi-square test with comparison to control group

Table 2. ***Apixaban pharmacokinetic parameters.***

	Control (*N*=12)	NAFLD (*N*=22)	*P*-value*	NAFLD No Fibrosis (*N*=11)	*P*-value*	NAFLD Fibrosis (*N*=11)	*P*-value*
$AUC_{0\text{-}12}$ (ng/mL×hr)	671 ± 174	545 ± 265	0.15	580 ± 228	0.30	511 ± 304	0.15
$AUC_{0\text{-}\infty}$ (ng/mL×hr)	840 ± 326	715 ± 351	0.31	725 ± 290	0.38	705 ± 417	0.40
C_{max} (ng/mL)	98 ± 31	78 ± 44	0.13	82 ± 40	0.33	74 ± 49	0.17
T_{max} (hr)	2.6 ± 1.1	2.7 ± 1.3	0.78	2.6 ± 1.1	0.96	2.8 ± 1.4	0.66
$t_{1/2}$ (hr)	4.5 ± 1.5	5.0 ± 1.2	0.34	4.5 ± 0.5	0.97	5.5 ± 1.4	0.12
$X_{urine,\ 0\text{-}12}$ (μg)	611 ± 148	544 ± 182	0.26	527 ± 176	0.23	562 ± 194	0.51
CL_{renal} (mL/min)	16.2 ± 5.4	19.6 ± 9.1	0.25	17.3 ± 8.5	0.71	21.8 ± 9.4	0.11

Mean ± S.D.; *two-tailed, t-test or Chi-square test with comparison to control group

DMD Fast Forward. Published on February 22, 2018 as DOI: 10.1124/dmd.117.079624
This article has not been copyedited and formatted. The final version may differ from this version.

Table 3. ***Multivariable linear regression analysis of apixaban AUC_{0-12}.***

Variable	Coefficient (95% C.I.)	*P-value*
Constant	1069 (608, 1529)	-
Weight (kg)	-7.97 (-11.76, -4.18)	<0.001
Age (yr)	2.16 (-4.21, 8.52)	0.49
NAFLD*	146 (-60, 352)	0.16
*CYP3A5*3*	6.7 (-142, 155)	0.93
ABCG2 421C>A	29.5 (-139.8, 198.8)	0.72

*Control = 0, NAFLD = 1; R^2 = 0.46

Table 4. ***Rosuvastatin pharmacokinetic parameters.***

	Control (***N*=12**)	**NAFLD** (***N*=22**)	***P*-value***	**NAFLD No Fibrosis** (***N*=11**)	***P*-value***	**NAFLD Fibrosis** (***N*=11**)	***P*-value***
$AUC_{0\text{-}12}$ (ng/mL×hr)	25.4 ± 11.0	20.1 ± 14.3	0.28	21.5 ± 13.5	0.46	18.6 ± 15.7	0.25
$AUC_{0\text{-}\infty}$ (ng/mL×hr)	30.7 ± 13.6	25.4 ± 17.0	0.35	27.0 ± 15.4	0.58	23.7 ± 19.2	0.36
C_{max} (ng/mL)	3.7 ± 2.0	3.0 ± 2.6	0.42	3.3 ± 2.6	0.70	2.8 ± 2.7	0.39
T_{max} (hr)	3.9 ± 2.0	3.8 ± 1.9	0.86	3.7 ± 2.1	0.81	3.9 ± 1.8	0.95
$t_{1/2}$ (hr)	4.4 ± 1.2	5.4 ± 2.9	0.21	4.8 ± 1.4	0.54	6.0 ± 4.0	0.25
$X_{urine,\ 0\text{-}12}$ (μg)	257 ± 107	209 ± 186	0.34	244 ± 230	0.87	174 ± 130	0.11
CL_{renal} (mL/min)	180 ± 64	178 ± 69	0.93	178 ± 84	0.94	178 ± 53	0.94

Mean ± S.D.; *two-tailed, t-test or Chi-square test with comparison to control group

DMD Fast Forward. Published on February 22, 2018 as DOI: 10.1124/dmd.117.079624
This article has not been copyedited and formatted. The final version may differ from this version.

Table 5. ***Multivariable linear regression analysis of rosuvastatin AUC_{0-12}.***

Variable	Coefficient (95% C.I.)	*P-value*
Constant	51 (24, 78)	-
Weight (kg)	-0.23 (-0.48, 0.01)	0.06
Age (yr)	-0.24 (-0.64, 0.16)	0.23
NAFLD*	3.0 (-10.5, 16.5)	0.65
SLCO1B1 521T>C	5.8 (-3.9, 15.6)	0.23
ABCG2 421C>A	-2.56 (-12.8, 7.7)	0.61

*Control = 0, NAFLD = 1; R^2 =0.23

DMD Fast Forward. Published on February 22, 2018 as DOI: 10.1124/dmd.117.079624
This article has not been copyedited and formatted. The final version may differ from this version.

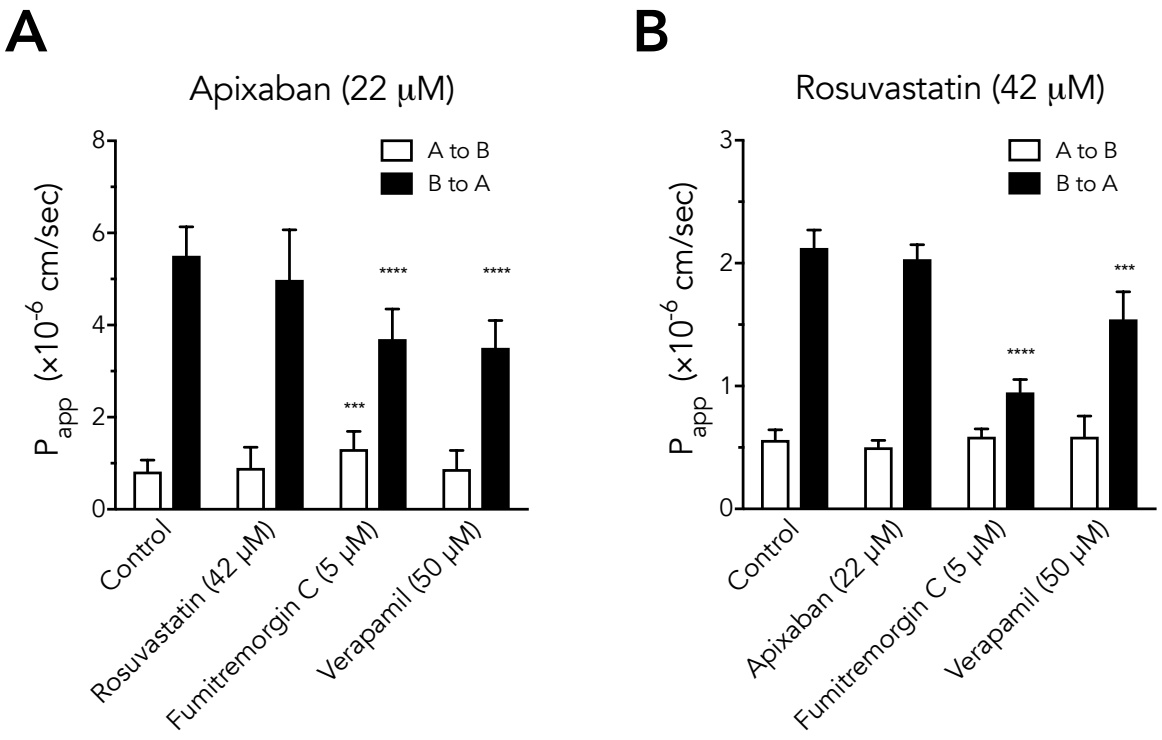

DMD Fast Forward. Published on February 22, 2018 as DOI: 10.1124/dmd.117.079624
This article has not been copyedited and formatted. The final version may differ from this version.

Figure 1.

DMD Fast Forward. Published on February 22, 2018 as DOI: 10.1124/dmd.117.079624
This article has not been copyedited and formatted. The final version may differ from this version.

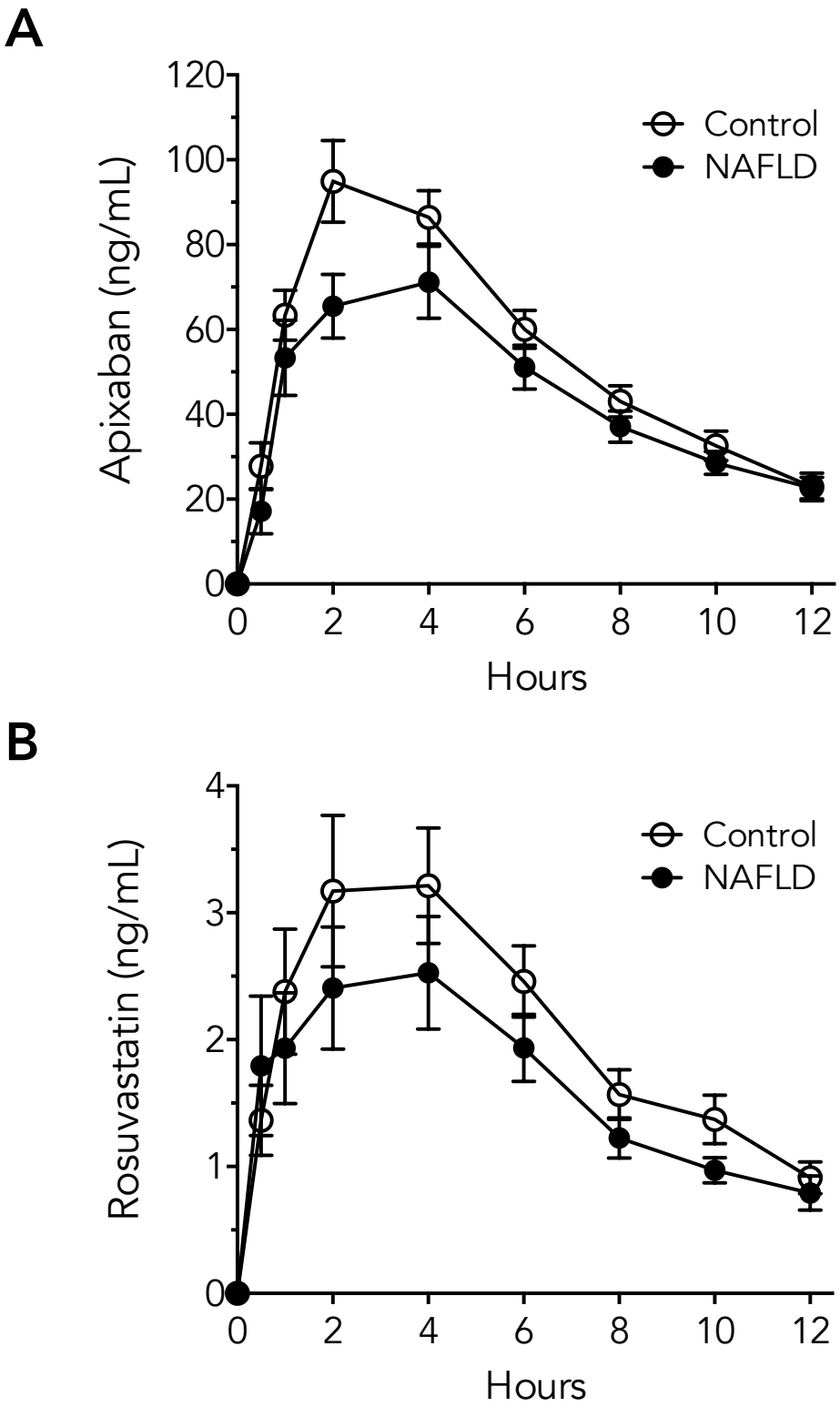

Figure 2.

DMD Fast Forward. Published on February 22, 2018 as DOI: 10.1124/dmd.117.079624
This article has not been copyedited and formatted. The final version may differ from this version.

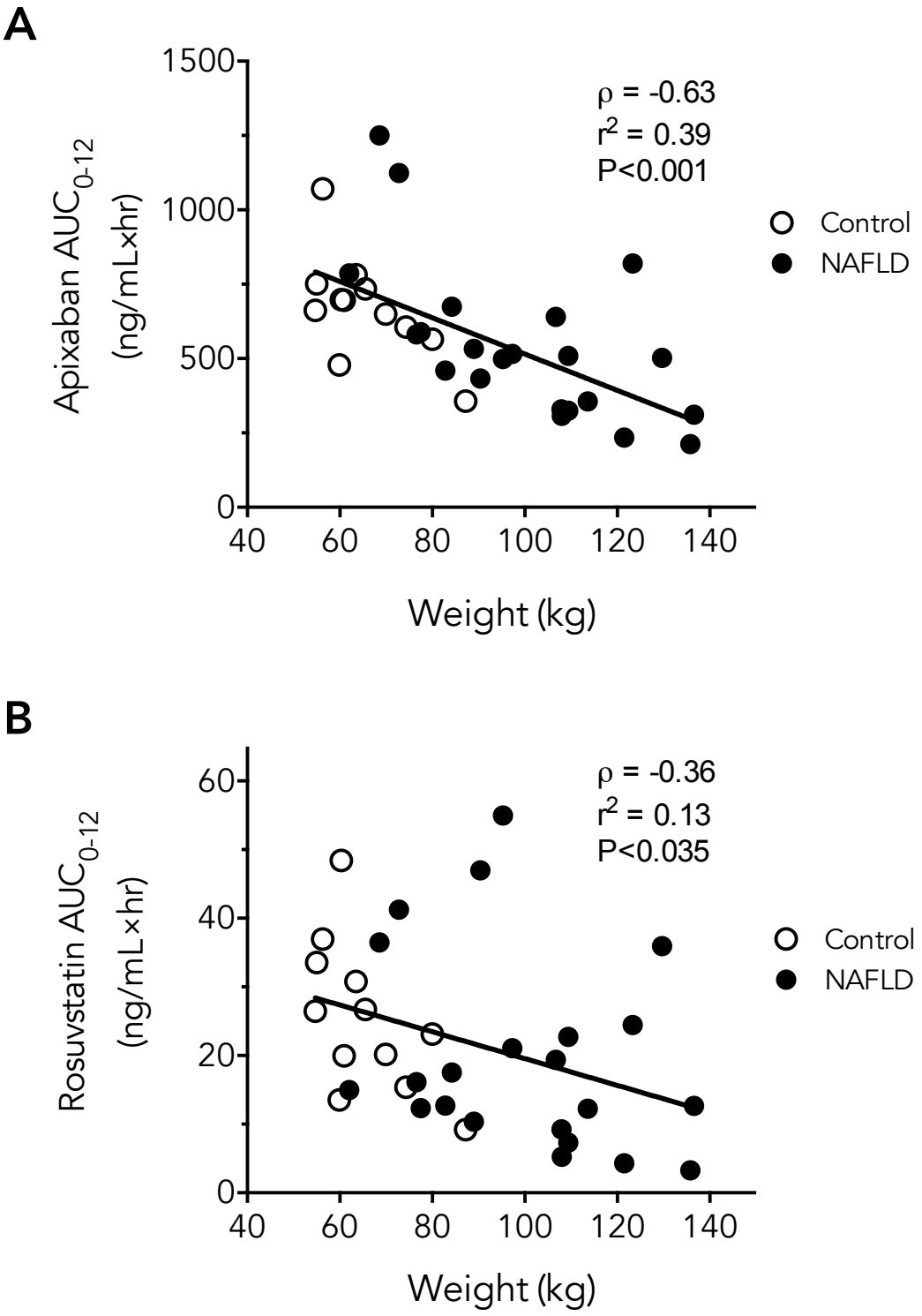

Figure 3.